



A HIGH-RESOLUTION MODELING TECHNIQUE OF IRREGULAR SUBSURFACE STRUCTURES USING H/V SPECTRAL RATIO OF LONG-PERIOD MICROTREMORS

Hirotoishi UEBAYASHI¹, Hidenori KAWABE² and Yoshihiro TAKEUCHI³

SUMMARY

One of the key problems in modeling the three-dimensional (3D) subsurface structure of sedimentary basins is extrapolation and/or interpolation from two-dimensional (2D) models constructed from reflection and refraction surveys. The use of microtremor horizontal-to-vertical (H/V) spectral ratios, allowing simple and quick microtremor measurements, may be suitable for this purpose. The validity and usefulness of long-period (>1s) microtremor H/V spectral ratios are investigated as a possible tool for extrapolation in 3D basin structure modeling.

Three-component microtremor observations were conducted at 51 stations located on three survey lines in the north of the Osaka basin, which encompasses the most complex geological structures in the basin. To reproduce these observations, 2D numerical simulations have been developed that account for the irregular shape of subsurface structures deduced from seismic reflection studies, microtremor array studies and deep drilling data. The 3D model obtained by combining the interpreted 2D subsurface structures is consistent with geological information for the area, such as surface geology and the location of active faults. Compared with the basement structure derived from the gravity prospecting, the proposed 3D model is more complicated, indicating a higher resolution than by the gravitational method.

The 3D numerical simulation of microtremors for the proposed 3D model is also conducted. It is indicated that in the synthetic H/V spectral ratios, it doesn't affect the predominant frequency though the wave-arrival direction of the microtremors affects the peak value. It is concluded that the proposed technique based on the microtremor H/V spectral ratio is a practical and useful means of extrapolating and interpolating irregular subsurface structures in 3D basin structure modeling.

¹ Assistant Professor, Hiroshima Intl. Univ., Hiroshima, Japan Email: ueba@it.hirokoku-u.ac.jp

² Research Associate, Research Reactor Inst., Kyoto Univ., Osaka, Japan

³ Professor, Hiroshima Intl. Univ., Hiroshima, Japan

INTRODUCTION

The development of numerical modeling methods and computing facilities has led to the simulation of strong ground motions in large-scale sedimentary basin (Uebayashi et al. [1], Graves [2], Sato et al.[3], Kamae and Kawabe [4]). One of the major obstacles remaining in the prediction of strong motions is the accurate modeling of three-dimensional structures of sedimentary basin. In Japan, following the Hyogo-ken-nanbu (Kobe) earthquake, many municipal governments conduct extensive surveys to construct 3-D subsurface structural models using reflection, refraction and microtremor array survey methods. However, these exploration methods are very expensive, and in many cases an insufficient number of survey lines were deployed within sedimentary basins. Therefore, interpolation of subsurface structure between survey lines becomes a serious problem. In this paper, the microtremor horizontal-to-vertical (H/V) spectral ratio is investigated as a tool for the extrapolation and interpolation of subsurface structures.

Exploration based on the H/V spectral ratio using single-station microtremor records is simple, quick, and inexpensive. Moreover, the microtremor H/V spectral ratio is stable over time (Nakamura [6]), being related to the predominant frequency of the Rayleigh-wave ellipticity curve (Nogoshi and Igarashi [7]). Based on this principle, irregular subsurface structures have been estimated from microtremor H/V spectral ratios (Yamanaka et al. [8], Tokimatsu et al. [9]). However, the reliability of the subsurface structural models estimated by these techniques is partially debatable because the Rayleigh-wave ellipticity curves are calculated on the basis of 1D horizontally stratified models. In this article, an irregular subsurface structure is used as a numerical models for synthesizing long-period (>1s) microtremors. The microtremor wavefields are synthesized by finite-element-method (FEM) for 2D case and finite-difference-method (FDM) for 3D case, respectively.

The irregular subsurface structural models are adjusted using the trial-and-error procedure so as to obtain agreement between observed and synthetic microtremor H/V spectral ratios at every measurement site. This technique is applied to the northern Osaka basin, called the Hokusetsu Area, an area that encompasses the most complex geological structures in the basin. We consider the cross-section derived from reflection survey as a reference for extrapolating subsurface structure, and then check the validity of the presented technique by comparing the estimated 3D model with geological information and gravity prospecting in this area.

SURFACE GEOLOGY OF HOKUSETSU AREA

Figure 1 shows a geological map and the distribution of microtremor observation sites in the Hokusetsu Area in the north of the Osaka Plain, Japan. The Hokusetsu Area is an important target for seismic disaster mitigation because the area includes key infrastructure and itself is a highly developed urban area. Senri hill located at the center of the Hokusetsu Area has been formed by the tectonic movement of faults (F1 to F4) having different strikes (Research Group of Active Faults in Japan [10]). The surface geology of the Hokusetsu Area can be roughly be classified into four types. The geology east and west of the hilly area consists of Osaka Group and terrace deposits. Recent alluvial deposits surround the hilly area, and the Tamba Group, which is the basement for the Hokusetsu Area, is distributed in the mountainous region to the

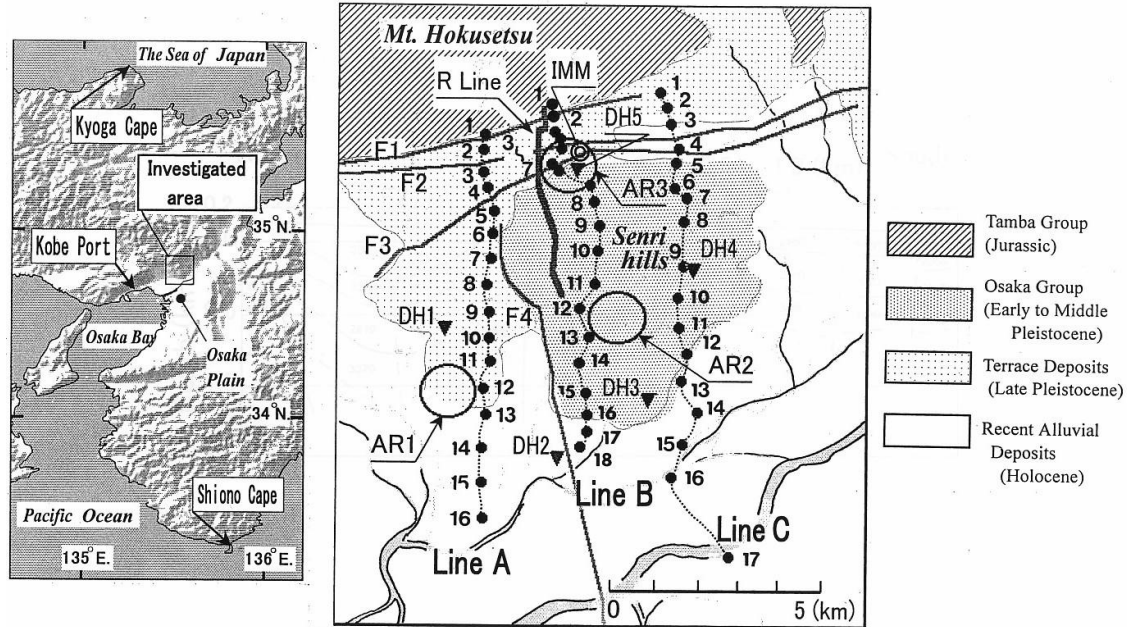


Figure 1. Maps of the Kinki region (left) in Japan and survey region (right) with surface geological conditions and active fault (F1 to F4). Arrows in the left map indicate ocean-wave-monitoring stations. On the right, solid circles denote the locations of microtremor measurement sites. Thick (R-) line denotes reflection survey. Open circles and inverted triangles denote the locations of microtremor array observations and deep drillings,

north. The inverted black triangles (DH1 to DH5) denote the locations of deep drilling for hot springs (Nakagawa et al. [11]), and the open circles (AR1 to AR3) denote the locations of microtremor array observations (Horike et al. [12]). These exploratory results will be used for verifying the subsurface structures extrapolated in this study. The locations of temporary microtremor measurements along three survey lines (A, B and C) are denoted by solid circles. During the temporary observations, continuous observations were taken at the IMM site denoted by the double circle. Figure 2 shows the cross section of the P-velocity structure below the R line shown in Figure 1, as interpreted by Horike et al. [12]. Between Senri hill and the Hokusetsu Mountains is a graben region of 2 to 3 km in width, sandwiched between the Arima-Takatsuki tectonic line (F1) and the Onohara fault line (F3).

MICROTREMOR OBSERVATION AND OCEAN WAVES

The average distance between temporary observation sites along each survey line was approximately 500 m. The lines A, B and C were observed in March, October, and December 2000, respectively. Each series of observations began at around 18:00 and concluded at around 5:00 the next morning. To locate the origin of long-period microtremors, spectral features of microtremors at IMM and ocean waves at the three monitoring stations indicated in Fig. 1 have been compared. Figure 3a shows a comparison between the fundamental predominant

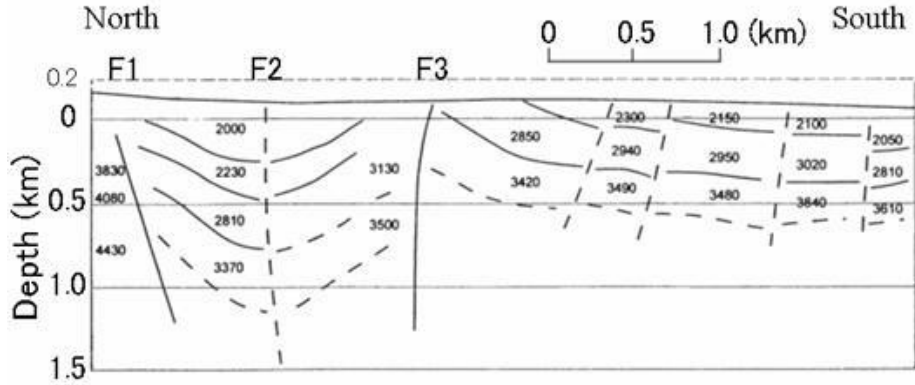


Figure 2. Cross-section of P-velocity structure below R-line interpreted from reflection survey (From Horike et al. [11]).

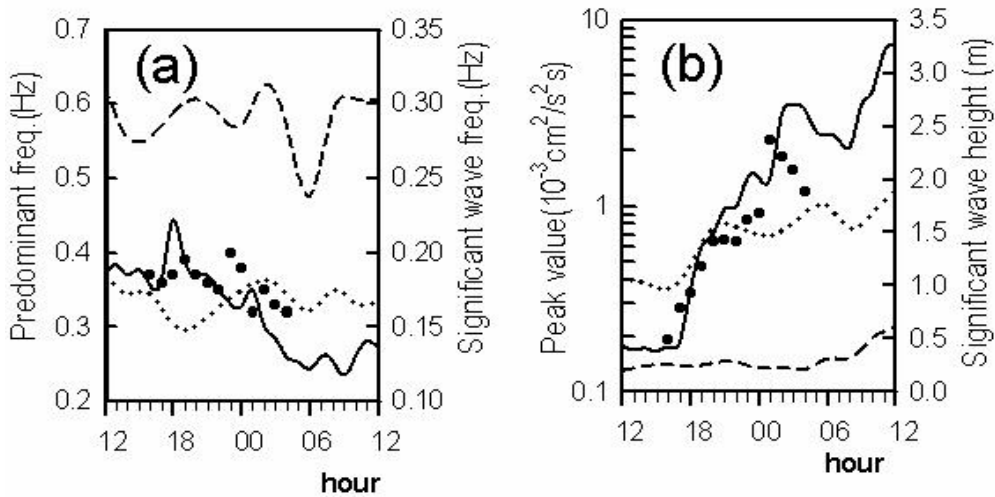


Figure 3. Comparison of between spectral features of microtremors at IMM and ocean waves at three monitoring station. Solid circles denote the predominant frequencies (a) and the peak values of H/V spectra (b). Solid, dotted, and short-dashed lines denote frequencies and wave heights of significant ocean waves at Kyoga, Siono and Kobe stations, respectively

frequencies of the vertical component in microtremor records and the significant ocean-wave frequencies. Figure 3b shows a comparison between the peak values of the power spectra in the microtremor records and the significant ocean-wave heights. These comparisons suggest that microtremors (solid circles) are more correlated with ocean-waves at Kyoga Cape (solid lines) than with those observed at Shiono Cape (dotted lines) and Kobe Port (dashed lines). In addition, the predominant frequencies are always twice the significant ocean-wave frequencies at Kyoga Cape (Longuet-Higgins [13], Uebayashi et al. [14]). From these results, the origin of long-period microtremors in the Hokusetsu Area can be estimated to be to the north, from the Sea of Japan. A similar result to these comparisons during observation on the line A has been obtained during other observations (lines B and C). The analytical process to obtain the microtremor H/V spectral ratio has been described in detail in Uebayashi [15].

REPRODUCTIONS OF H/V SPECTRAL RATIO BY 2D AND 3D SIMULATIONS

Overview of Spatial Variation of Observed H/V Spectral Ratio

The spectral ratios were obtained for two sets of north-south component to vertical component (H_{NS}/V) and east-west component to north-south component (H_{EW}/H_{NS}) in microtremor records. As an overview of the spatial variation of these spectral ratios, Figure 4 show contour maps depicting the relationships between spectral ratios and location for the three survey lines. In the maps of H_{NS}/V (Figure 4a), the following three features were identified: 1) the predominant frequency gradually decreases toward the south (right) on Lines A and C. On Line B, the frequency changes quickly from 0.5 to 0.4 Hz in the region (B13 to B16) between the hilly area (B9 to B12) and alluvial area (B17 and B18). 2) At observation sites 8 to 16, the predominant frequency is about 0.1 Hz lower on Line A than on Line C. 3) The spectra have broad peaks in areas of strong irregularity, such as the hilly edges (broken outline). In the maps of H_{EW}/H_{NS} (Figure 4b), on the other hand, the EW-component of microtremor amplitude parallel to the gutter of the graben becomes larger than the NS-component orthogonal to the gutter (solid outline). From our recent research, the anisotropy of amplitude concerning the two horizontal components is revealed not only in microtremors but also in seismic motions. This phenomenon may be attributed to the subsurface structure. Therefore, to clarify the phenomenon, we will discuss from the result of the 3D microtremor simulation in the later section.

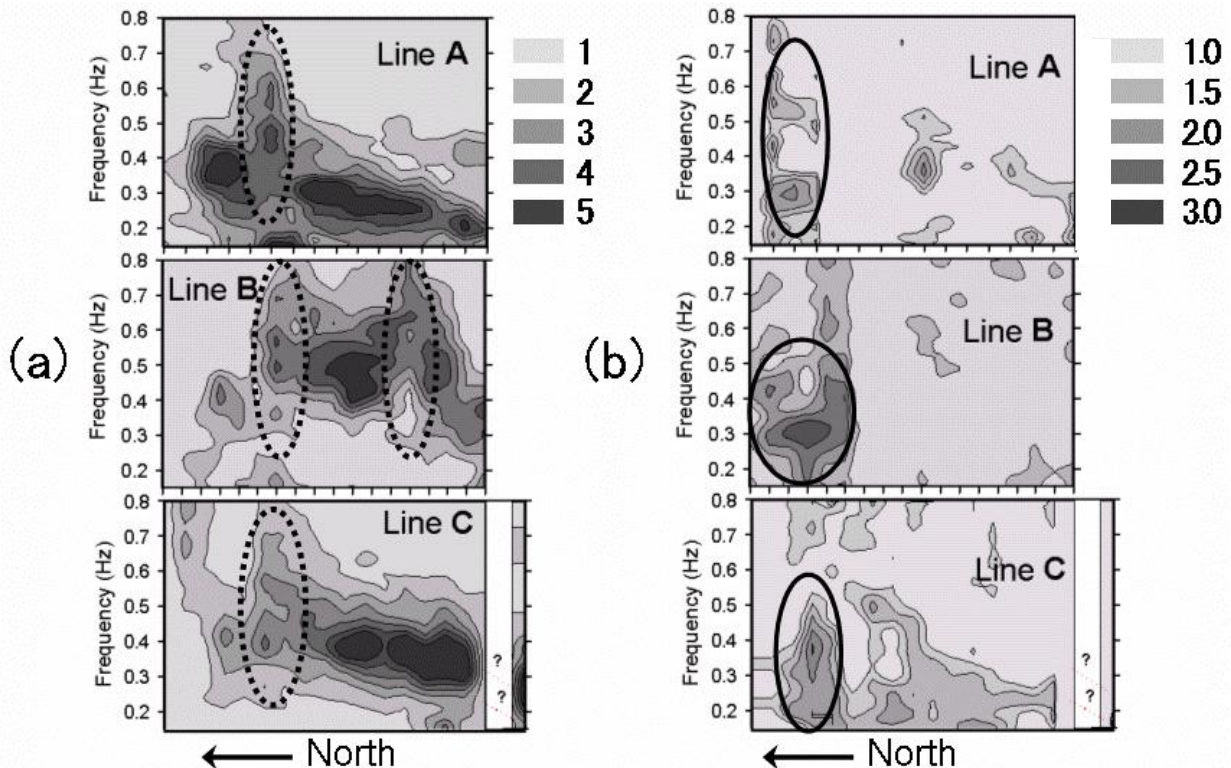


Figure 4. Contour maps depicting the relationships between the spectral ratios and the locations for three survey lines. The left (a) and the right (b) show the spectral ratios of north-south component to vertical component (H_{NS}/V) and east-west component to north-south component (H_{EW}/H_{NS}), respectively.

2D Numerical Modeling for Synthesizing Long-Period Microtremors

The investigated region below the three survey lines, 11.2 km wide and 1.6 km deep, is embedded in the horizontally stratified bedrock region (120 km wide, 28 km deep). The element size is 66.7 m square in the investigated region and 800 m square in the horizontally stratified region. A viscous boundary condition is set at the bottom of this model and an energy-transfer boundary condition is set at each of the two sides. Numerical simulations of long-period microtremors were made using 2D FEM (JKK, [16]).

The origins of microtremors are dealt with as line sources (i.e., an in-plane problem) distributed at random intervals from 1 to 5 km on the ground surface about 90 to 110 km north from the target area. Five excitation points were set, each assigned vertical excitation forces. In this study, the process for obtaining the source time function related to the excitation forces is not important because the items related to the source time function are cancelled implicitly in the spectral ratio.

Extrapolation from the cross section (corresponding to B1 to B12) interpreted by the reflection method shown in Figure 2 was executed for the subsurface structure in the same plane (B13 to B18) as its section and out-of-plane (Lines A and C). The initial S-velocity structure of the reference cross-section (B1 to B12) is decided by the S-velocity profile derived from microtremor array observation at AR2. The initial models of the extrapolated cross-sections were decided on the basis of the spatial variation of predominant frequency at the H/V spectral ratios shown in Figure 4a.

Comparison of Simulated and Observed H/V Spectral Ratios

The subsurface structural models were adjusted so as to obtain agreement of the H/V spectral ratios at every observation site between observations and FEM calculations. As a result, we obtained three cross-sections of the subsurface structure, as shown in Fig. 5. Figure 6 shows the spatial variations of the H/V spectral ratios derived from numerical simulations to be compared with the observed results in Figure 4a. The comparisons indicate that the numerical simulations closely reproduce the three features in the observed results described in the previous section.

The influence of the irregularities on the H/V spectral ratio at typical observation sites is illustrated in Figure 7, showing the theoretical H/V spectral ratios derived from the FEM models (bold black solid lines), the observed H/V spectral ratios (gray solid lines), and Rayleigh ellipticity curves for fundamental and first-higher modes derived from the 1D stratified models (fine and broken lines). These comparisons of H/V spectral ratios at all observation sites have been shown in Uebayashi [15]. The 1D models match the stratigraphic columns beneath each observation site in the 2D models. The sites can be roughly classified into the following three groups based on the coincidence of the observational and the theoretical curves: 1) R1 denotes a site where the 1D models, 2D models, and observation results all match with respect to the fundamental predominant frequency and its peak value; 2) R2 denotes a site where the 2D models and observation results match with respect to the broad peaks near the fundamental predominant frequencies, but differ from the 1D models, exhibiting sharp peaks; and 3) R3 denotes a site where the 2D models and observation results match well with respect to the spectral shape across a wide frequency band, but differ from the 1D models with regard to the fundamental predominant frequency and spectral shape. The colored bars above each cross-section in Figure 5 denote the classification in these three groups. Considering the relationships between these classifications and the inferred subsurface structures, R1 (blue) denotes a horizon-

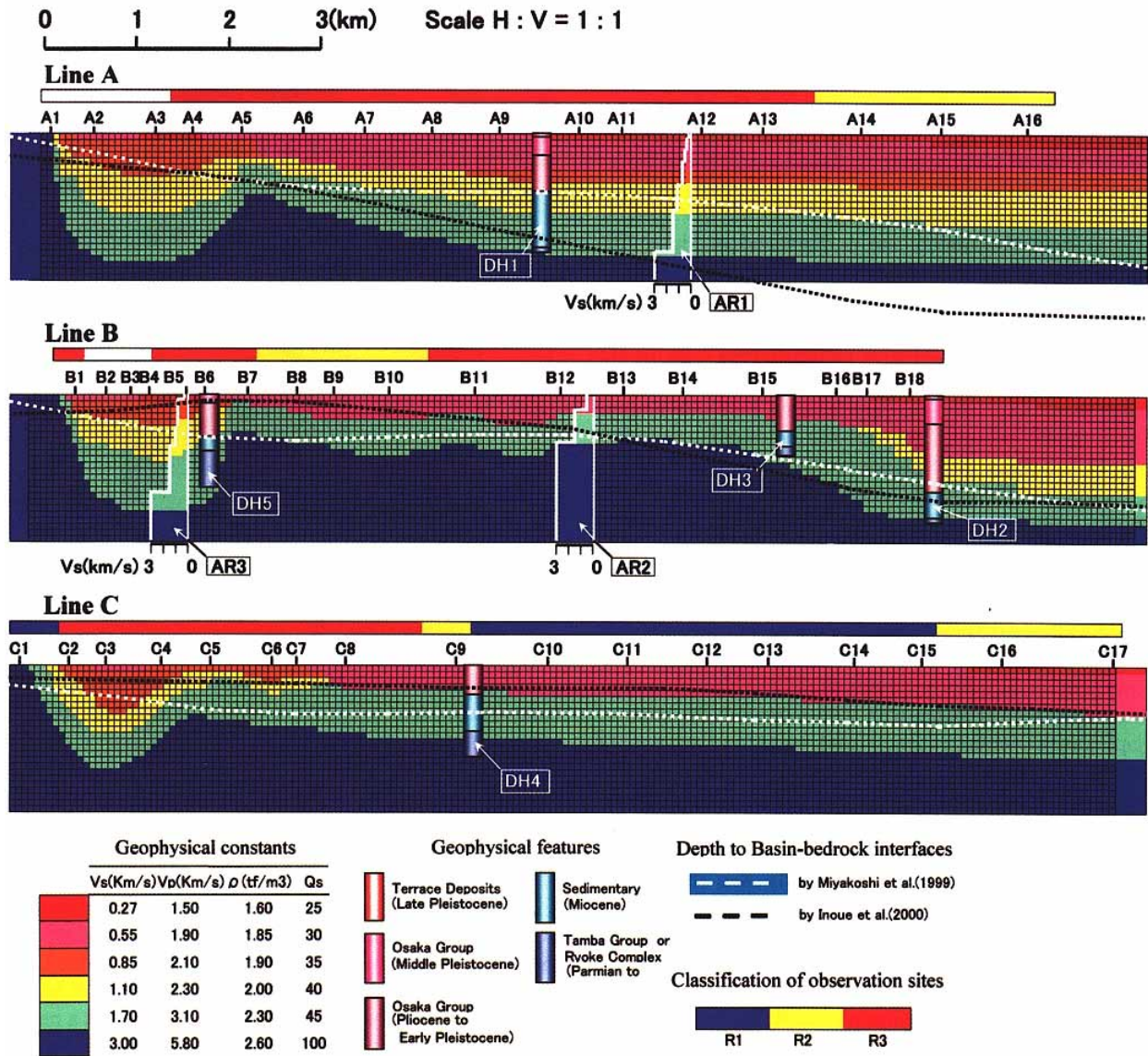


Figure 5. Interpreted irregular subsurface structures at cross sections below survey lines A, B and C. These models are compared with geological profiles derived from other prospecting techniques. The colored bars above each cross-section denote the classification of each observation site based on the coincidence of observational and theoretical curves of H/V ratios.

tally stratified region away from a strongly irregular region, R2 (yellow) rather denotes a horizontally stratified region close to a strongly irregular region or a slightly inclined region at a basin-bedrock interface, and R3 (red) denotes a strongly irregular region.

As shown in Figure 7, the observed H/V spectral ratios of A3 and A5 in the graben are larger than those given by the 2D models over a broad frequency band. The exclusion of 3D effects may have been the cause of the discrepancy between observations and the 2D simulations. Moreover, presented 2D simulations imply the assumption that the microtremors regarded as coherent wave motions come from a specific direction (i.e. north). These problems will be clarified from the 3D simulation of microtremors in the next section.

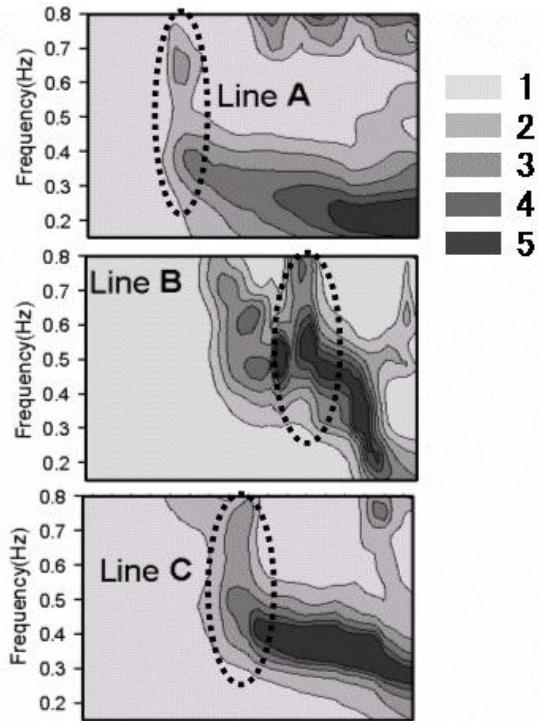


Figure 6. The same as Figure 4a, but for 2D numerical simulations for interpreted structures shown in Figure 5.

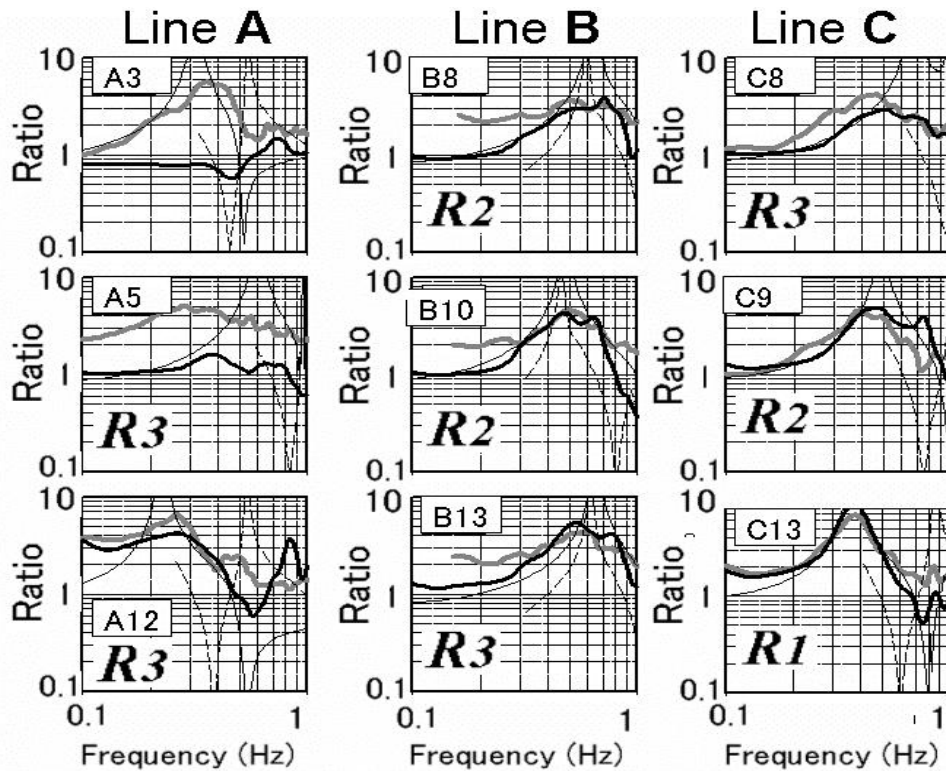


Figure 7. Comparison of theoretical H/V spectral ratios derived from the FEM models (bold black solid lines), Rayleigh ellipticity curves for fundamental and first-higher modes derived from the 1D stratified models (fine and broken lines) with observed H/V spectral ratios (gray solid lines).

3D Numerical Simulation of Long-Period Microtremors

Figure 8 shows the configuration of the basin-bedrock interface of the 3D subsurface structural model constructed by interpolating and extrapolating from the interpreted 2D subsurface structures at cross-sections below the survey lines A, B and C. The FDM (Graves [2], Pitarka [17]) was applied in the microtremor syntheses for the 3D model. The model is 159km long (N90°E), 92km wide and 28km deep. The investigated region (Figure 8), 13.6km long, 13.2km wide and 2km deep, is located at the south end of the model. A grid spacing of 0.08km in the investigated region is used, which gives a frequency resolution limit of 1.0Hz within the lowest velocity layers (0.55km/s) of the model. The number of grid points is 470×345×90, the time increment is 0.006s, and the number of time step is 19000. The origins of microtremors dealt with as point sources are distributed from the northwestward to the northeastward at most equal intervals. Five vertical-excitation points were set on the ground surface at a distance 80km away from the target area. The procedure so as to obtain the simulated H/V spectral ratios is the same as that of the 2D FEM simulation introduced in previous section.

The comparisons of the H/V spectral ratio obtained for each of two horizontal components between the FDM calculation (blue lines) and the observation (red lines) are shown in Figure 9. The H/V spectral ratios of the FDM calculation are corresponding with that of the observation, as shown in Figure 9a. In Figure 9b showing the comparison at the site B5 in the graben, on the other hand, it is a change for the better than the previous 2D simulation though the reproductions of the H/V spectral ratio by the 3D simulation are unsatisfactory. In the both of the simulation and the observation at site B5, the spectral value in the vicinity of predominant frequency of the H_{EW}/V is twice that of the H_{NS}/V . This result suggests that it is reproduced by this 3D simulation that the amplitude of the EW-component is greater than that of the NS-component as mentioned previously.

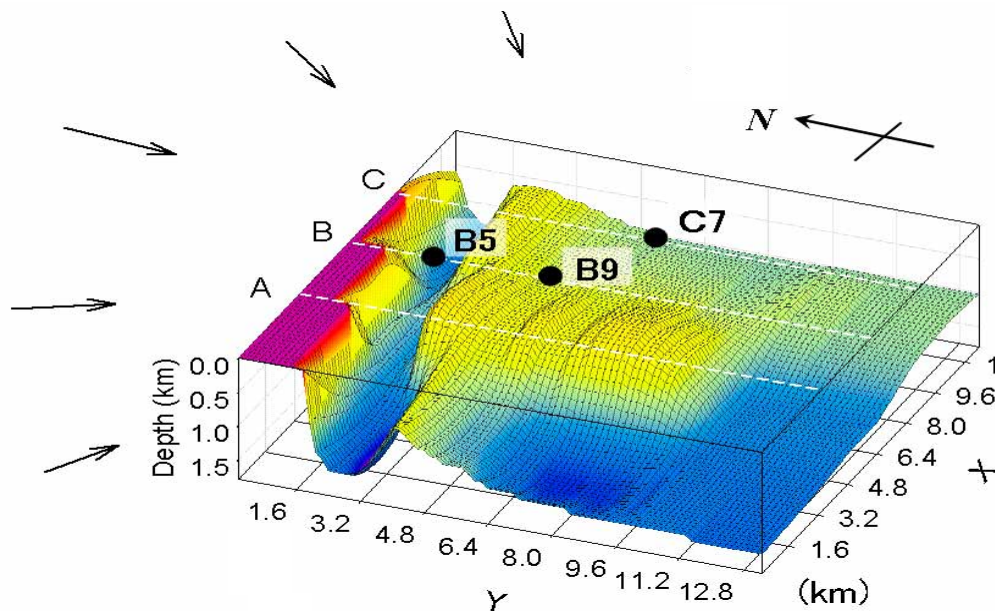


Figure 8. Configuration of the basin-bedrock interface of the 3D subsurface structural model constructed by interpolating and extrapolating from the interpreted 2D subsurface structures at cross-sections below the survey lines A, B and C.

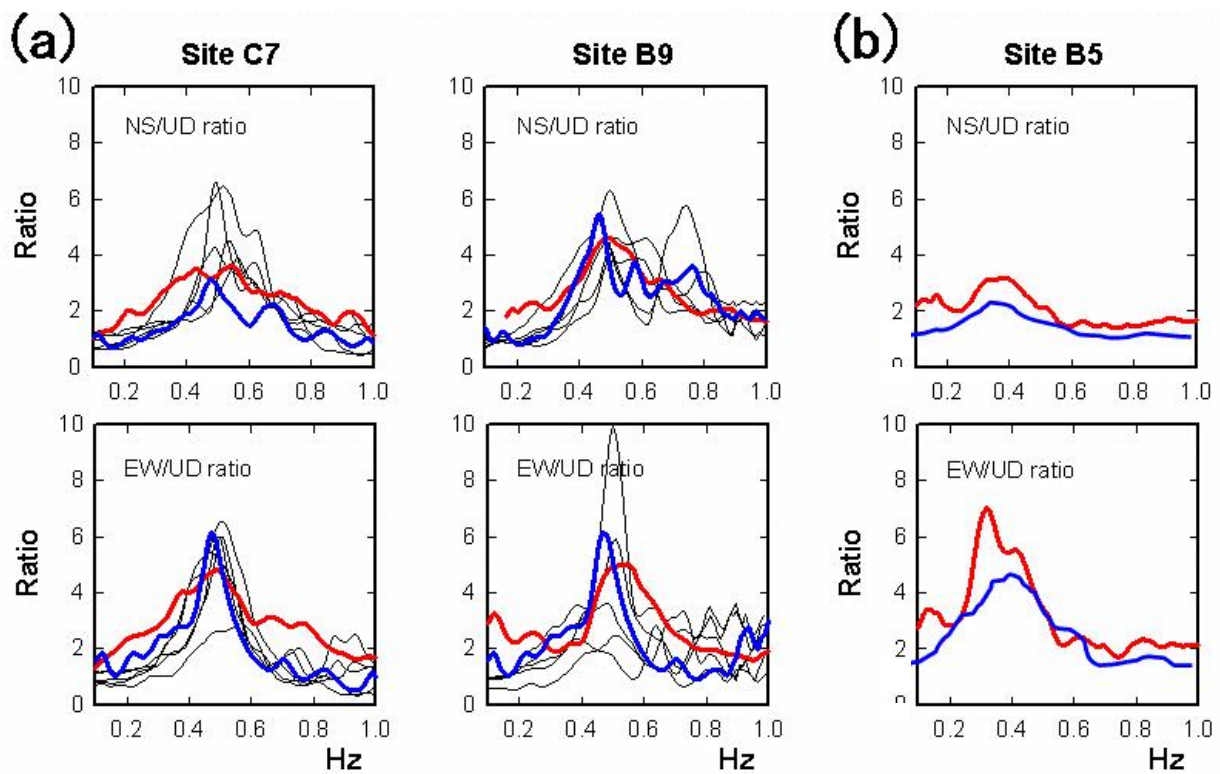


Figure 9. Comparisons of H/V spectral ratios obtained for each of two horizontal components between 3D simulation (blue lines) and observation (red lines). The H/V spectral ratios (fine black lines) calculated for each of the five excitation points are also shown in Figure 9a.

To investigate the effects of the wave-arrival direction of microtremors, the H/V spectral ratios (fine black lines) calculated for each of the five excitation points are also shown in Figure 9a. It can be indicated from those black lines that it doesn't affect the predominant frequency though the wave-arrival direction of the microtremors affects the peak value of the H/V spectral ratios. The blue lines showing the H/V spectral ratio in the case excited at five points simultaneously show roughly the mean about those black lines.

VERIFICATION OF ESTIMATED IRREGULAR SUBSURFACE STRUCTURE

To verify the estimated subsurface structural models, geological profiles derived from deep drillcores at DH1 to DH5 and the S-velocity profiles at AR1 to AR3 inferred from microtremor phase velocities are included in Figure 5. The estimated models agree well with those profiles with regard to the depth to the basin-bedrock interface and to the internal boundaries, except for AR3. The estimated subsurface structure in the graben under line B does not agree with the S-velocity profiles at AR3. The reliability of the profile estimated from microtremor array observation based on 1D horizontally stratified model is debatable because the local area around

AR3 is an extremely irregular structure. The depth of the basin-bedrock interface derived from microtremor array observation at AR3 is similar to that averaged in the range from sites B1 to B7. This result suggests that the basement depth derived from microtremor array observation at AR3 is shallower than that estimated by this study at site B5.

The basement depth in the hilly area along Line A (A6 to A13), the westernmost line, is about 300 to 800 m deeper than that along the other survey lines (B8 to B15 and C5 to C14). This supports the inference that the basement below Line A is positioned on the footwall side of dip-slip fault F4, as shown in Figure 1, and is therefore deeper. The above-mentioned results indicate that the 3-D model obtained by the proposed technique is also consistent with the basement structure inferred from the location of active faults.

The distribution of basement depth in the entire Osaka Plain has been inferred from the gravity prospecting (Inoue et al. [18]) and various geophysical and geological surveys (Miyakoshi et al. [19]). In Figure 5, the broken black and broken white lines denote these two exploration results. These lines also agree with the estimated models in that the basement depth increases globally from the northern mountainous area to the southern plain area, excepting the graben area. However, the basement depths indicated by those broken lines are shallower than that of the estimated models in all areas, and the broken lines are too smooth to resolve the strong irregularities to the north and south of the hilly area. These results imply that the estimated models are more detailed and complex, indicating higher resolution than that achieved based on the gravity prospecting.

CONCLUDING REMARKS

The validity and usefulness of long-period microtremor H/V spectral ratios have been investigated as a tool for the extrapolation to model 3D basin structures. Three-component microtremor observations were conducted in the north of the Osaka basin, the geologically most complex area in the basin, and the microtremor H/V spectral ratios were inferred. Numerical simulations of long-period microtremors were made using 2D FEM and 3D FDM. Taking into account the 2D subsurface structure obtained by reflection surveys, irregular subsurface structural models were adjusted so as to obtain agreement between the observations and the simulations at every site with respect to the H/V spectral ratios. The following results were obtained from a comparison of the subsurface structural models obtained by the proposed technique and the other existing techniques for modeling subsurface structure. The 3D model obtained by the proposed technique agreed well with geological profiles derived from deep drillcores and microtremor array observations at several points. Compared with the basement structure derived from the gravity prospecting, the proposed 3D model is more complicated, indicating a higher resolution than by the gravitational method. From these results it is concluded that the proposed technique is a practical and useful means of extrapolating and interpolating irregular subsurface structures in 3D basin structure modeling.

By comparing Rayleigh ellipticity curves based on 1D stratified models with observed H/V spectral ratios, the following three areas could be characterized. 1) In areas located far from strongly irregular regions, approximated as horizontally stratified regions, the fundamental predominant frequencies and peak values agree. 2) In areas located near strongly irregular regions, also approximated by a horizontally stratified region, the fundamental predominant

frequencies agree but the peak values do not. 3) In areas above strongly irregular regions, both the fundamental predominant frequencies and peak values differ markedly.

The following results were obtained from the 3D numerical simulation of microtremors for the 3D subsurface structural model inferred from the proposed technique. It doesn't affect the predominant frequency of H/V spectral ratio through the wave-arrival direction of microtremors affects the peak value of H/V spectral ratio. The anisotropy of amplitudes concerning the two horizontal components of microtremors was attributed to the irregularities of subsurface structures, such as the graben.

ACKNOWLEDGMENTS

I am grateful to Dr. Masanori Horike of Osaka Institute of Technology for suggesting this problem, for valuable advice, and for improvement of the manuscript. I am also indebted to many former undergraduate students, who performed and processed extensive microtremor measurements. I would also like to thank Naoko Kitada, Naoto Inoue, Takao Kagawa, and Ken Miyakoshi of Geo-Research Institute supplied the geological information. I am also grateful to Dr. Takekazu Udaka and Mr. Osamu Uchida of Jishin Kogaku Kenkyusho Inc. for their help in the computer programs. This study is supported in part by the Grant-in-Aid for Scientific Research (No.12750522 and No.11792026) from Japan Society of the Promotion of Science.

REFERENCES

1. Uebayashi, H., M. Horike, and Y. Takeuchi (1992). Seismic motion in three-dimensional arbitrarily-shaped sedimentary basin, due to a rectangular dislocation source, *J. Phys. Earth*, 40, 223-240.
2. Graves, R.W. (1996). Simulating seismic wave propagation in 3D elastic media using staggered grid finite differences, *Bull. Seism. Soc. Am.*, 86, 1091-1106.
3. Graves, R.W. (1998). Three-dimensional finite-difference modeling of the San Andreas fault: Source parameterization and ground-motion level, *Bull. Seism. Soc. Am.*, 88, 881-897.
4. Sato, T., R.W. Graves, and P. G. Somerville (1999). Three-dimensional finite-difference simulations of long-period strong motions in the Tokyo Metropolitan Area during the 1990 Odawara earthquake (Mj5.1) and the Great 1923 Kanto earthquake (Ms 8.2) in Japan, *Bull. Seism. Soc. Am.*, 89, 579-607.
5. Kamae, K and H. Kawabe (2002). Prediction of broad-band strong ground motions from large subduction earthquake using a characterized source model, AGU Fall meeting, S12B-1214.
6. Nakamura, Y. (1989). A method for dynamic characteristics estimation of subsurface using microtremor on the ground surface, *QR of RTRI*, 30, 25-33.
7. Nogoshi, M. and T. Igarashi (1971). On the amplitude characteristics of microtremors (Part2), *Zisin (J. Seism. Soc. Japan)* 24, 26-40 (in Japanese with English abstract).
8. Yamanaka, H., M. Takemura, H. Ishida, and M. Niwa (1994). Characteristics of long-period microtremors and their applicability in exploration of deep sedimentary layers, *Bull. Seism. Soc. Am.* 84, 1831-1841.

9. Tokimatsu, K., H. Arai, and Y. Asaka (1996). Three-dimensional soil profiling on Kobe area using microtremors, in Proc. 10th World Conf. Earthquake Eng. #1486, Elsevier Science Ltd.
10. Research Group of Active Faults in Japan(1991). Active faults in Japan revised edition, Univ. Tokyo Press(in Japanese).
11. Nakagawa, K., K. Ryoki, N. Muto, S. Nishimura, and K. Ito (1991). Gravity anomaly map and inferred basement structure in Osaka Plain, Central Kinki, South-west Japan, J. Geosci. Osaka City Univ. 34, 103-117.
12. Horike, M., Y. Takeuchi, T. Fujita, A. Kowada, T. Ikawa, and T. Kawanaka (1998). Survey of the subsurface structure of the boundary region between the Hokusetsu mountains and the Osaka basin, Zisin (J. Seism. Soc. Japan) 51, 181-191 (in Japanese with English abstract).
13. Longuet-Higgins, M. S. (1950). A theory of the origin of microseisms, Phil. Trans., Roy. Soc. London A243, 1-35.
14. Uebayashi, H., S. Sakai, A. Hasegawa, Y. Tanaka, and Y. Maeda (1996). Spatial variation of microtremors in Nada and Higashinada wards, Japan, Effect of time-variation of ocean waves, Summ. Techn. Papers Annu. Meeting Architectural Inst. Japan B1, 229-230.(in Japanese with English abstract).
15. Uebayashi, H. (2003). Extrapolation of irregular subsurface structures using the horizontal-to-vertical spectral ratio of long-period microtremors, Bull. Seism. Soc. Am., 93, 570-582.
16. Jishi Kogaku Kenkyusho Inc. and Kozo Keikaku Eng. Inc. (2000). Super FLUSH/2D for Windows, Ver2.00 (Analytical program for 2-D dynamic soil-structure interaction, Store purchased: udaka@flush.co.jp or uchida@flush.co.jp).
17. Pitarka, A. (1999). 3D elastic finite-difference modeling of seismic motion using staggered grids with nonuniform spacing, Bull. Seism. Soc. Am., 89, 54-68.
18. Inoue N. and K. Nakagawa (2000). Modeling of the underground structure in the Osaka sedimentary basin based on geological interpretation of gravity anomalies and seismic profiles, J. Geosci. Osaka City Univ. 43, 97-110.
19. Miyakoshi, K., T. Kagawa, B. Zhao, M. Tokubayashi, and S. Sawada (1999). On the modeling of deep sedimentary structure beneath the Osaka plain (part3), in Summ. Japan Earth Planetary Scie. Joint Meeting #Sh-009 (in Japanese with English abstract).